

# The three-dimensional evolution of a plane wake

By H. Maekawa,<sup>1</sup> R. D. Moser<sup>2</sup> AND N. N. Mansour<sup>2</sup>

## 1. Introduction

In the past three decades, linear stability analysis has led to a comprehensive understanding of the linear stages of transition in plane wakes. Our understanding of the nonlinear and turbulent stages is less developed. Nonlinear theory developed by Papageorgiou & Smith (1988) was used to study the long-wavelength regime in wakes. The nonlinear and turbulent stages have been investigated experimentally, and few numerical studies have examined the early nonlinear stages of forced wakes.

Experimental studies of the wake have been carried out extensively by Sato & Kuriki (1961), Sato & Onda (1970), Sato & Saito (1975, 1978), and Gharib & Williams-Stuber (1989). Sato & Onda (1970) reported that the wake responds differently under different kinds of forced disturbances. Gharib & Williams-Stuber (1989) investigated the enhancement and cancellation of perturbations in a plane wake by the strip heater technique. They showed that the mean velocity profile adjusts itself to become more receptive to the forced frequency.

In their numerical study, Maekawa, Mansour & Buell (1992, hereafter referred to as MMB), simulated spatially developing plane wakes with inlet forcing using a single frequency (fundamental mode), a fundamental mode with its subharmonics and random perturbations. They found that phase jitter around the fundamental frequency plays a critical role in generating vortices of random shape and spacing. They also observed pairings and doublets in the wake. These observations were similar to those reported by Comte, Lesieur & Chollet (1989) and by Aref & Siggia (1981) for temporally developing layers. Furthermore, MMB found that infinitesimal random disturbances generate clear alternate-signed vortex streets due to selective amplification of the fundamental mode.

The formation of three-dimensional structures and turbulent breakdown are not as well understood. Chen, Cantwell & Mansour (1990) showed that the phase between a two-dimensional fundamental mode and oblique modes controls the formation of three-dimensional structures in plane wakes. Depending on the phase, loop-like structures were observed. These structures were similar to the flow visualization experiments by Breidenthal (1980), Meiburg & Lasheras (1988), Antonia, Brown & Bisset (1987), and Perry, Lim & Chong (1980). However, a detailed understanding of the underlying mechanism that initiates three-dimensional breakdown in wakes and the resultant structure is still missing.

In what follows, the evolution of three dimensional disturbances in a incompressible wake is investigated using direct numerical simulations. The instantaneous three-dimensional structures and corresponding statistics are presented.

1 University of Electro-Communications, Chofu, Tokyo 182

2 NASA Ames Research Center, 202A-1, Moffett Field, California 94035

## 2. Preliminaries

The time-developing mixing layer code used by Rogers & Moser (1992) was modified to accommodate wake profiles. The cases described in this study are initialized with controlled initial conditions. We consider temporally evolving layers where the flow is taken to be periodic in  $x$ - and  $z$ - (streamwise and spanwise) directions. The cross-stream direction,  $y$ , is taken to be doubly infinite with boundary conditions applied at  $x = \pm\infty$ . The length of the computational domain in the streamwise and spanwise directions,  $L_x$  and  $L_z$ , is set to be integer multiples of the perturbation wavelength. Thus, in general,  $L_x = n\lambda_x$  and  $L_z = m\lambda_z$ .  $n$  and  $m$  are one or two for all cases reported here. The Reynolds number defined by the half-width and the deficit velocity of the wake is 300. As was done in MMB, the flow structure and various flow statistics were examined for a range of Reynolds numbers,  $100 \leq Re \leq 600$ . The observed variations with  $Re$  indicate that  $Re = 300$  is large enough to eliminate low-Reynolds number effects.

### 2.1 The governing equations and numerical considerations

The simulations reported here were performed by solving the vorticity equation derived from the incompressible Navier-Stokes equations:

$$\frac{\partial \omega}{\partial t} + \nabla \times (\omega \times U) = \frac{1}{Re_0} \nabla^2 \omega, \quad (1)$$

where  $Re_0 = U_0 b_{1/2} / \nu$  ( $\nu$  is the kinematic viscosity) is the Reynolds number,  $b_{1/2}$  is the initial half-width of the wake, and  $U_0$  is the centerline deficit velocity. All quantities are non-dimensionalized by the appropriate characteristics scale,  $U_0$  and  $b_{1/2}$ .

The spectral Galerkin method described by Spalart, Moser & Rogers (1991) was used for spatial discretization. The equations were advanced in time using a compact third-order Runge-Kutta scheme. A typical three-dimensional simulation ( $n = 1, m = 1$ ) required  $48 \times 64 \times 48$  Fourier/Jacobi modes.

### 2.2 Specification of initial conditions

The initial mean velocity used for all the simulations reported here is of the form

$$\bar{U} = \exp \left( -\ln(2) \left( \frac{y}{b_{1/2}} \right)^2 \right) \quad (2)$$

which has a half width of  $b_{1/2}$ . In addition to the mean flow, simple perturbations are included in the initial conditions.

To specify the initial conditions and facilitate discussion through this paper, it is necessary to refer to specific wavenumbers; they will be referred to in ordered pairs

$$(\alpha, \beta) = \left( \frac{k_x \lambda_x}{2\pi}, \frac{k_z \lambda_z}{2\pi} \right) \quad (3)$$

where  $\lambda_x$  and  $\lambda_z$  are the  $x$  and  $z$  wavelengths from linear stability theory,  $k_x$  and  $k_z$  are corresponding wavenumbers. The fundamental modes discussed here have  $\alpha$  and/or  $\beta$  equal to one. The amplitude  $A_{\alpha\beta}$  of a Fourier mode  $(\alpha, \beta)$  is defined to be the square root of the integrated (in  $y$ ) energy in that mode, as described in Rogers & Moser (1991).

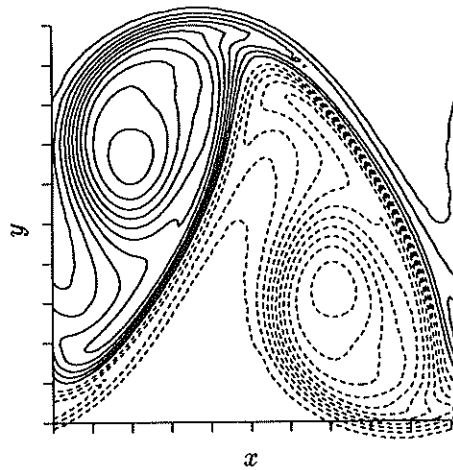


FIGURE 1. Spanwise vorticity structure of the two-dimensional wake (Case 2D-1) at the first maximum of  $A_{10}$  ( $t = 48$ ). Contour increments are 0.05 and tic marks are at  $b_{1/2}$  intervals.

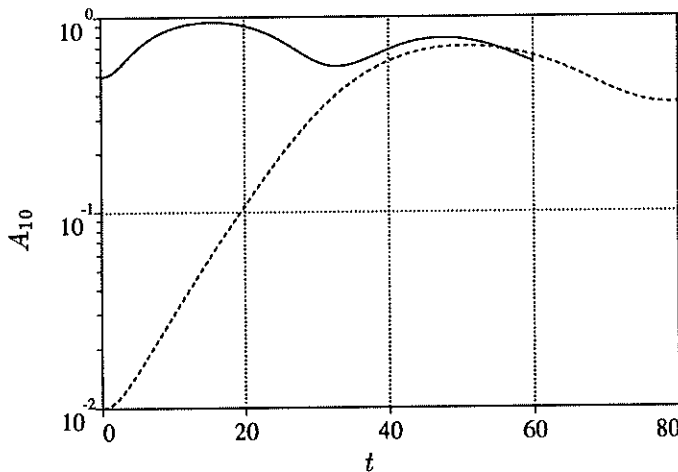


FIGURE 2. Time development of the two-dimensional fundamental mode amplitude for — Case 2D-2 (high initial amplitude) and ---- 2D-1 (low amplitude).

### 3. Accomplishments

#### 3.1 Two-dimensional simulations

To facilitate discussion of the three-dimensional evolution of the wake, we start by briefly reexamining the behavior of two-dimensional wakes. The spatially developing simulations of MMB showed that the growth of the fundamental mode is responsible for the formation of the vortex street in wakes. We consider three different initial conditions for the current two-dimensional simulations. Case 2D-1 starts with a

single fundamental mode with small amplitude ( $A_{10} = 0.01$ ), Case 2D-2 starts with a single fundamental mode with large amplitude ( $A_{10} = 0.5$ ), and Case 2D-3 starts with a fundamental mode and its first subharmonic with large amplitudes ( $A_{\frac{1}{2}0} = A_{10} = 0.5$ ).

As in the spatially developing case, the amplitude of the fundamental grows exponentially, then saturates. Contours of spanwise vorticity at the time when the amplitude of the fundamental disturbance,  $A_{10}$ , reaches its maximum are shown in Figure 1 for Case 2D-1. The vortices evident in this figure have an oblong or elliptical shape, with the major axis roughly vertical. Successive snapshots show that the structures rotate by  $90^\circ$  so that the major axis is horizontal, consistent with the observations of MMB. If we define the rollup time  $t_r$  to be at the first maximum of the fundamental disturbance amplitude, we find for this case,  $t_r = 48$ .

When a larger initial amplitude is used (Case 2D-2), the fundamental mode saturates sooner ( $t_r = 18$ ). After saturation, the mode loses energy at a much faster rate than in Case 2D-1, then starts growing again, and a second maximum appears (see Figure 2). The orientation of the major axis of the vortical structure at the first maximum of  $A_{10}$  ( $t_r = 18$ ) is similar to the low-amplitude case. But as the structure rotates its major axis toward the horizontal, a tail of weak vorticity is formed (see Figure 3 at  $t = 32$ ). Successive snapshots show that the vortices continue to rotate, becoming vertical again when  $A_{10}$  reaches a second maximum. This is similar to the observations by MMB of active structures at higher Reynolds number.

In Case 2D-3, we observe (see Figure 4) pairing of negative sign vorticity (in the lower portion of the layer) and shredding of positive sign vorticity (in the upper portion). The development time of the subharmonic is slow relative to the fundamental, and pairing occurs around the time when the amplitude of the subharmonic reaches its maximum.

### *3.2 Three-dimensional wake*

To study the sensitivity of the two-dimensional wake to initial (or inlet) three-dimensional disturbances, five cases were studied: two cases (Case 3D-1, and Case 3D-1-1) where a two-dimensional mode plus background random noise of different amplitudes are used for initial conditions, and three cases with a two-dimensional mode and a pair of oblique modes (Case 3D-2-1, Case 3D-2-2 and Case 3D-2-3) of different amplitudes for initial disturbances. The relative phase between the two-dimensional mode and the oblique modes was kept the same at  $\pi/4$  for all cases.

The intent in Case 3D-1 is to mimic the experiment of Sato & Onda (1970) where a fundamental mode is forced, but, as in all experiments, background noise exists. Figure 5(a) shows the evolution of  $A_{10}$  for Case 2D-1 and 3D-1. Clearly the weak background noise in this case has little effect on the evolution of the two-dimensional layer. The structure that dominates in this case is the two-dimensional double roller. In this case, the fastest growing three-dimensional modes are those whose wave-numbers are closest to that of the two-dimensional fundamental. Large amplitude disturbances were used in Case 3D-1-1 ( $A_{10} = 0.1$ , average amplitude of three-dimensional modes of 0.025). In this case, a band of wave numbers around the fundamental are enhanced after the roll-up. But, the energy in the subharmonic

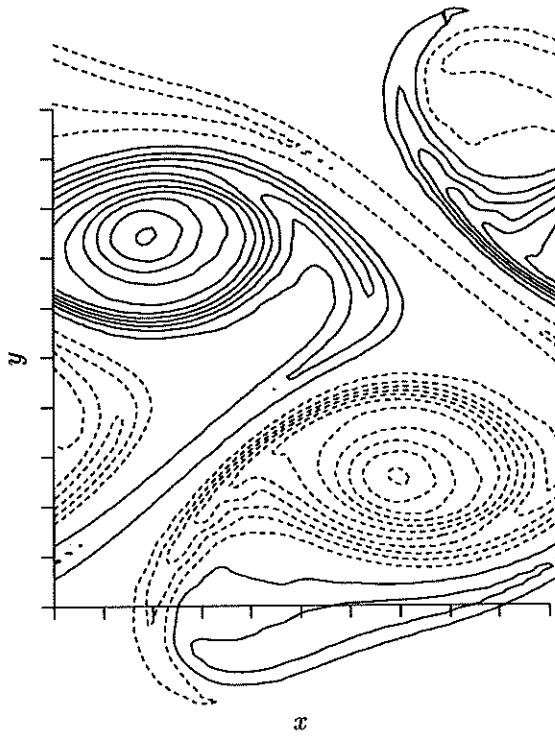


FIGURE 3. Spanwise vorticity in Case 2D-2 at  $t = 32$ ; contour increments are 0.09 and tic marks are at  $b_{1/2}$  intervals.

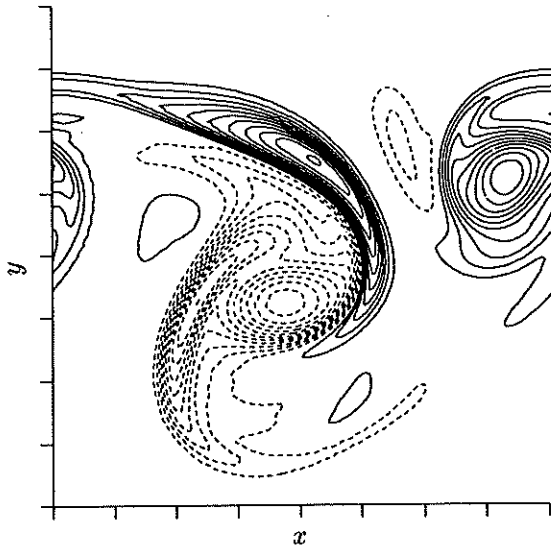


FIGURE 4. Spanwise vorticity in Case 2D-3 during pairing/tearing. Contour increments are 0.05 and tic marks are at  $2 \times b_{1/2}$  intervals.

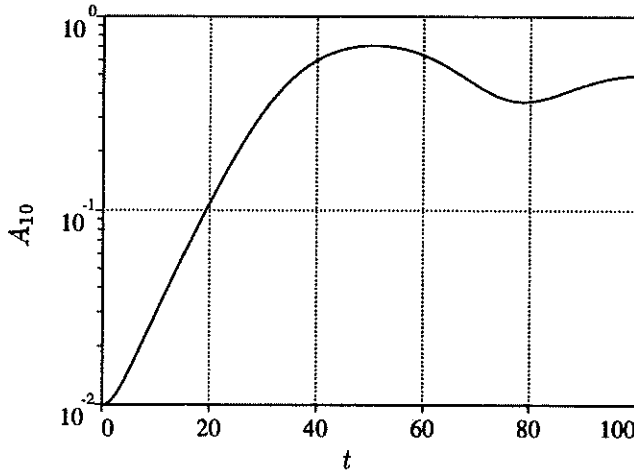


FIGURE 5. Evolution of the two-dimensional fundamental mode amplitude in — 3D-1 and ---- 2D-1 (plots on top of 3D-1 case).

mode decreases after the rollup, suggesting that pairing in the wake is not as natural as in the mixing layer. But as seen in our two-dimensional simulations, it will occur when forced. The vortex structure in case 3D-1-1 is again dominated by the two-dimensional vortices.

The results of the previous two cases suggest that low-wavenumber oblique modes are not amplified during the rollup of the fundamental structure in the wake. We thus use a relatively small spanwise wavelength ( $\lambda_z = 0.6\lambda_x$ ) for the forced oblique modes as in Rogers & Moser (1992). The three oblique cases; Case 3D-2-1, 3D-2-2 and 3D-2-3 have initial amplitudes such that  $A_{10} > A_{11}$ ,  $A_{10} < A_{11}$ , and  $A_{10} = A_{11}$  respectively.

In Case 3D-2-1, the evolutions of the mode amplitudes indicate that the two-dimensional mode grows, saturates, and decreases while the energy in the oblique modes reaches a first peak at the same time as the fundamental ( $t = 14$ ) but later continues to increase until a second maximum is reached at  $t = 30$ . At this time, the oblique mode amplitude is at almost the same level as the fundamental. Constant spanwise vorticity surfaces for this case at  $t = 14$  and  $t = 30$  are shown in Figure 6. In Figure 6(a), the core rolls are apparent but are surrounded by 'wisps' of vorticity that form hoop-like structures. Later ( $t = 30$ ) after the oblique modes grow (at  $t = 30$ ) we find that the strong spanwise vorticity is concentrated in compact regions (Figure 6(b)). At this time, the streamwise and the cross-stream components of the vorticity dominate the large scale structures. The counter-rotating vortices shown in Figure 6(c) become the dominant feature of the flow. Of the three vorticity components,  $\omega_y$  is largest in magnitude, while  $\omega_z$  is smallest. The vortex structures are inclined at 40 to 50 degrees with respect to the streamwise direction. These streamwise vortex pairs are reminiscent of the rib vortices in the plane mixing layer.

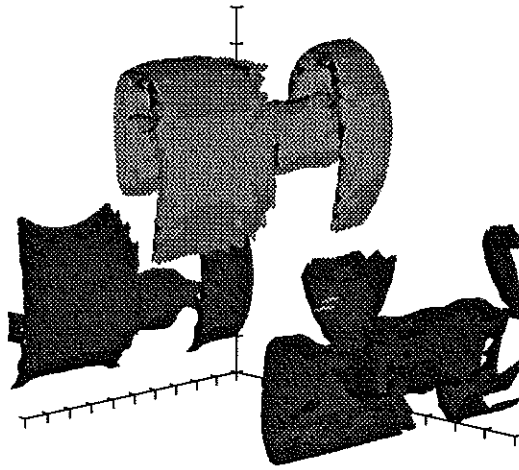


FIGURE 6(a). Three-dimensional structure of spanwise vorticity in Case 3D-2-1 at  $t = 14$ : Surfaces represent 50% of peak value ( $\pm 2.6$ ), and tic marks are  $b_{1/2}$  intervals.

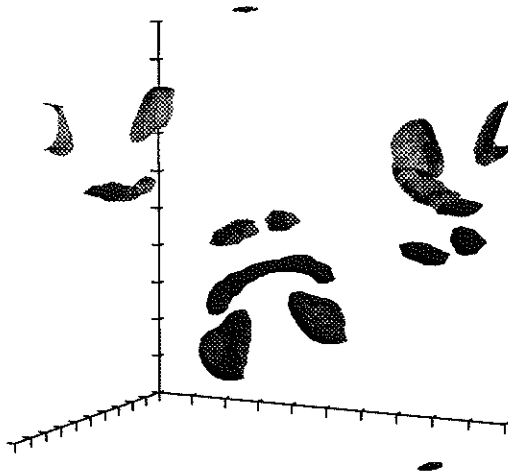


FIGURE 6(b). Three-dimensional structure of spanwise vorticity in Case 3D-2-1 at  $t = 30$ : Surfaces represent 50% of peak value ( $\pm 1.6$ ), and tic marks are  $b_{1/2}$  intervals.

When the oblique modes are initially dominant (Case 3D-2-2), it was found that they grow rapidly and suppress the growth of the two-dimensional fundamental mode. Since the oblique modes are larger than the two-dimensional mode, the spanwise vorticity structure is not observed in the wake. When all the modes have the same amplitude (Case 3D-2-3), the energy in the modes indicates that the oblique modes and the fundamental mode grow together and that the oblique mode saturates first, then the fundamental modes saturate.

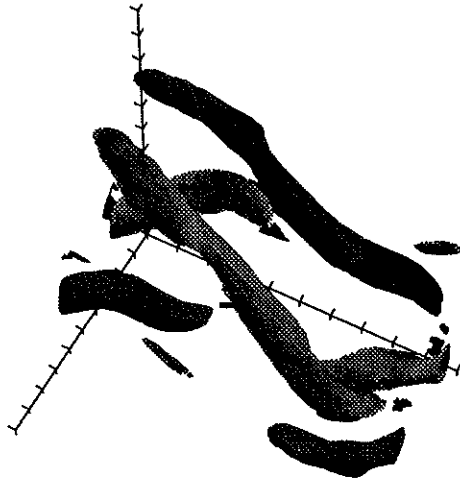


FIGURE 6(c). Three-dimensional structure of streamwise vorticity in Case 3D-2-1 at  $t = 30$ : Surfaces represent 50% of peak value ( $\pm 1.9$ ), and tic marks are  $b_{1/2}$  intervals.

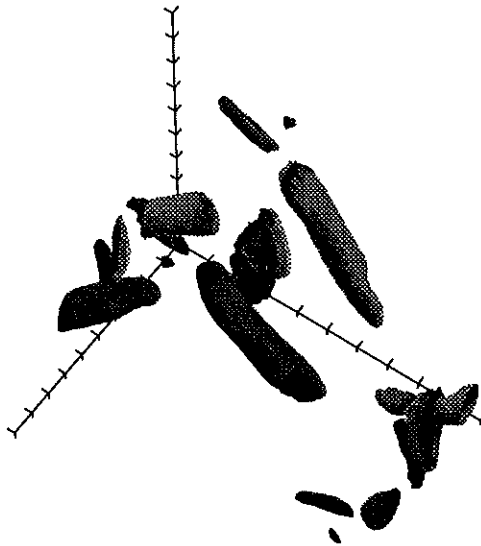


FIGURE 6(d). Three-dimensional structure of  $\omega_y$  in Case 3D-2-1 at  $t = 30$ : Surfaces represent 50% of peak value ( $\pm 2.6$ ), and tic marks are  $b_{1/2}$  intervals.

#### 4. Conclusions

Direct numerical simulations have been used to study the three-dimensional evolution of a plane wake. The flow has been analyzed by visualizing the vortical structures using vorticity contours and by tracking the modal energy in time. The two-dimensional features are similar to the results obtained for a two-dimensional spatially developing wake (MMB).



The growth of fundamental mode generates characteristic alternating sign vortices in the wake. When a two-dimensional fundamental mode is forced with high amplitude, vortical structures with 'wisps' around the roller are generated. When the wake is forced with a fundamental and a subharmonic asymmetric pairing and shredding are observed.

When weak three-dimensional random disturbances are imposed in addition to a two-dimensional fundamental mode, we find that the two-dimensional rollers appear to be the dominant features of the wake. Analysis of the energy contained in each mode reveals that three-dimensional modes with wavenumber close to that of the two-dimensional fundamental mode grow after saturation of the fundamental mode. In contrast, the energy in the low wavenumbers modes decreases.

When the wake is forced with oblique modes of various amplitudes, we find that at large amplitudes the growth of the oblique mode leads to the breakdown of the alternate-sign vortex structures in the wake, and counter-rotating streamwise vortical structures are generated after the breakdown. These streamwise structures are inclined at 40 to 50 degrees with respect to the streamwise direction. When the amplitude of the initial oblique modes is higher than that of the fundamental, the growth of the fundamental mode is suppressed, and no spanwise coherent structures were found in this case.

### Acknowledgements

The first author (H. M.) wishes to acknowledge the hospitality of the Center for Turbulence Research during the course of this work.

### REFERENCES

- ANTONIA, R., BROWNE, W. & BISSET, D. 1987 A description of the organized motion in the turbulent far wake of a cylinder at low Reynolds number. *J. Fluid Mech.* **184**, 423.
- AREF, H. & SIGGIA, E. D. 1981 Evolution and breakdown of a vortex street in two dimensions. *J. Fluid Mech.* **109**, 435.
- CHEN, J. H., CANTWELL, B. J. & MANSOUR, N. N. 1990 The effect of Mach number on the stability of a plane supersonic wake. *Phys. Fluids, A*, **2**, -(6), 984.
- COMTE, P., LESIEUR, M. & CHOLLET, J. P. 1989 Numerical simulations of turbulent plane shear layers. *Turbulent Shear Flows*. **6**, 360-380.
- GHARIB, M. & WILLIAMS-STUBER, K. 1989 Experiments on the forced wake of an airfoil. *J. Fluid Mech.* **208**, 225-255.
- MAEKAWA, H., MANSOUR, N. N. & BUELL, J. C. 1992 Instability mode interactions in a spatially developing plane wake. *J. Fluid Mech.* **235**, 223-254.
- MEIBURG, E. & LASHERAS, J. 1988 Experimental and numerical investigation of the three-dimensional transition in plane wakes. *J. Fluid Mech.* **190**, 1.

- MOSER, R. D. & ROGERS, M. M. 1992 The three-dimensional evolution of a plane mixing layer: paring and transition to turbulence. *submitted to J. Fluid Mech.*
- PAPAGEORGIU, D. T. & SMITH, F. T. 1989 Nonlinear instability of the wake behind a flat plate place parallel to a uniform stream. *Proc. R. Soc. Lond. A.* **419**, 1-29.
- PERRY, A., LIM, T. & CHONG, J. 1980 The instantaneous velocity fields of coherent structures on coflowing jets and wakes. *J. Fluid Mech.* **101**, 243.
- PIERREHUMBERT, R. T. & WIDNALL, S. E. 1982 The two- and three-dimensional instabilities of a spatially periodic shear layer.. *J. Fluid Mech.* **114**, 59-82.
- ROGERS, M. M. & MOSER, R. D. 1992 The three-dimensional evolution of a plane mixing layers: the Kelvin-Helmholtz rollup. *J. Fluid Mech.* **243**, 183-226.
- SPALART, P. R., MOSER, R. D. & ROGERS, M. M. 1991 Spectral methods for the Navier-Stokes equations with one finite and two periodic directions. *J. Comput. Phys.* **96**, 297-324.
- SATO, H. & KURIKI, K. 1961 The mechanism of transition in the wake of a thin flat plate placed parallel to a uniform flow. *J. Fluid Mech.* **11**, 321-352.
- SATO, H. & ONDA, Y. 1970 Detailed measurements in the transition region of a two-dimensional wake. *Inst. Space & Aero. Sci., Univ. Tokyo Rep.* **453**, 317-377.
- SATO, H. & SAITO, H. 1975 Fine-structure of energy spectra of velocity fluctuations in the transition region of a two-dimensional wake. *J. Fluid Mech.* **67**, 539-559.
- SATO, H. & SAITO, H. 1978 Artificial control of the laminar turbulent transition of a two-dimensional wake by external sound. *J. Fluid Mech.* **84**, 657-672.